molecules

MDPI

Article

Metabolic Profiling for Unveiling Mechanisms of Kushenol F against Imiquimod-Induced Psoriasis with UHPLC/MS Analysis

Xingxin Yang [1,†], Jiaoli Cheng [2,†], Xunqing Yin [1], Ting Ao [1], Xudong He [1], Yaqin Yang [3,*], Yuping Lin [1,*] and Zhen Chen [2,*]

[1] College of Pharmaceutical Science, Yunnan University of Chinese Medicine, Kunming 650500, China; yxx78945@163.com (X.Y.); yinxunqing1018@163.com (X.Y.); ace153790@163.com (T.A.); hexudong@ynutcm.edu.cn (X.H.)
[2] Science and Technology Achievement Incubation Center, Kunming Medical University, Kunming 650500, China; jiaoli_cheng980217@163.com
[3] School of Pharmaceutical Sciences, Zhejiang Chinese Medical University, Hangzhou 311403, China
* Correspondence: rc.yaqin0902@zcmu.edu.cn (Y.Y.); linyuping1221@163.com (Y.L.); chenzhen@kmmu.edu.cn (Z.C.); Tel.: +86-571-86633177 (Y.Y.); +86-871-65933303 (Y.L.)
† These authors contributed equally to this work.

Abstract: Psoriasis is a common chronic immune-mediated inflammatory skin disorder. *Sophora flavescens* Alt. (*S. flavescens*) has been widely acknowledged in the prevention and treatment of psoriasis. Kushenol F (KSCF) is a natural isopentenyl flavonoid extracted from the root of *S. flavescens*. We aimed to investigate the effect and mechanism of KSCF on imiquimod (IMQ)-induced psoriasis-like skin lesions in mice. A mouse model of psoriasis was induced with 5% IMQ for 5 days, and the mice were given KSCF dermally for 5 days. Changes in skin morphology, the psoriasis area, the severity index (PASI), and inflammatory factors of psoriasis-like skin lesions were evaluated. Metabolites in the psoriasis-like skin lesions were analyzed with ultra-high-performance liquid chromatography/mass spectrometry followed by a multivariate statistical analysis to identify the differential metabolites and metabolic pathway. The results of the present study confirmed that KSCF significantly reduced PASI scores, epidermal thickening, and epidermal cell proliferation and differentiation. KSCF also reduced the levels of interleukin (IL)-1β, IL-6, IL-8, IL-17A, IL-22, IL-23, and tumor necrosis factor (TNF)-α in the injured skin tissues while increasing IL-10 content. KSCF significantly regulated metabolites in the skin samples, and a total of 161 significant metabolites were identified. These differential metabolites involved sphingolipid and linoleic acid metabolism and steroid hormone biosynthesis. Collectively, KSCF inhibited the inflammatory response to prevent IMQ-induced psoriasis-like skin lesions in mice by call-backing the levels of 161 endogenous metabolites and affecting their related metabolic pathways. KSCF has the potential to be developed as a topical drug for treating psoriasis symptoms.

Keywords: inflammation; Kushenol F; psoriasis; metabolomics; *Sophora flavescens*

check for updates

Citation: Yang, X.; Cheng, J.; Yin, X.; Ao, T.; He, X.; Yang, Y.; Lin, Y.; Chen, Z. Metabolic Profiling for Unveiling Mechanisms of Kushenol F against Imiquimod-Induced Psoriasis with UHPLC/MS Analysis. *Molecules* **2024**, *29*, 2410. https://doi.org/10.3390/molecules29112410

Academic Editor: José Rubén Tormo

Received: 16 March 2024
Revised: 26 April 2024
Accepted: 17 May 2024
Published: 21 May 2024

Copyright: © 2024 by the authors. Licensee MDPI, Basel, Switzerland. This article is an open access article distributed under the terms and conditions of the Creative Commons Attribution (CC BY) license (https://creativecommons.org/licenses/by/4.0/).

1. Introduction

Psoriasis is a chronic and systemic immune-mediated disease. The underlying pathomechanisms involve an interplay between the innate and adaptive immune systems [1,2]. Recently, psoriasis presents many challenges, including high prevalence, chronicity, and associated comorbidity [3]. As a representative inflammatory skin disease occupied by large surface involvement, the occurrence and development of psoriasis is reported to be related to the disorder of many inflammation markers, such as IL-17A, IL-23, and TNF-α. Biologics targeting IL-17A, IL-23, and TNF-α have been developed and approved for the treatment of psoriasis [4]. The progression of psoriasis has also been confirmed to be related to immunity [5–7].

Common treatments for psoriasis include topical agents, systemic therapy, and ultraviolet light therapy. Topical agents mainly include calcipotriol (CVD), corticosteroids, and salicylic acid. Methotrexate, cyclosporine, and acitretin are commonly used as systemic therapy for psoriasis [8,9]. Although the therapeutic effects of these drugs have been widely recognized, adverse reactions still largely limit their clinical utilization [10]. Hence, complementary and alternative medicine may offer options for some patients.

Sophora flavescens Alt. (*S. flavescens*) is widely used in the clinic, can clear dampness-heat, kill insects, and dispel wind evil, which originates from the teachings of traditional Chinese medicine [11]. *S. flavescens* has been clinically used in numerous countries to treat skin diseases [12,13]. Kushenol F (KSCF) is a natural isopentenyl flavonoid extracted from the root of *S. flavescens*. It has been reported to have anti-inflammatory and anti-bacterial properties [14–16]. A previous study demonstrated that KSCF oral treatment could be an important therapeutic for treating atopic dermatitis. Although various studies have reported the biological effects of KSCF, the effect and mechanism of KSCF on psoriasis are unclear.

Metabolomics can reveal the specific changes in physiological and biochemical states related to phenotypes in biological systems. The application of skin metabonomics is suitable for revealing the potential functional changes in a variety of metabolic pathways and signal networks in psoriasis-like organisms, which has become a significant approach to evaluate the efficacy and mechanism of drugs [17]. The present study investigated the effects of KSCF on imiquimod (IMQ)-induced psoriasis-like skin lesions in mice using conventional pharmacology and metabolomics. The potential biomarkers and complex mechanisms of KSCF involved in psoriasis treatment are also discussed. The results demonstrated that KSCF inhibited the inflammatory response to prevent IMQ-induced psoriasis-like skin lesions in mice by call-backing the levels of 161 endogenous metabolites and affecting their related metabolic pathways. Thus, KSCF has the potential to be developed as a topical drug for treating psoriasis symptoms.

2. Results and Discussion

2.1. KSCF Mitigated the Psoriatic Dermatitis Induced by IMQ

Psoriasis is a skin disease with characteristics of well-demarcated, erythematous, raised lesions with silvery-white dry scales. As depicted in Figure 1, after 5 days of IMQ treatment, erythema and silvery-white dry scales were observed on the dorsal skin, and the PASI was significantly increased ($p < 0.001$). However, after treatment with CVD and KSCF, the thickness and size of the scales on the dorsal skin were decreased. Erythema and PASI were also significantly decreased ($p < 0.001$). These results indicate that KSCF effectively relieved IMQ-induced psoriasis symptoms.

2.2. Effect of KSCF on Inflammatory Reactions in Psoriasis-like Mice

Psoriasis is a chronic inflammatory skin disease characterized by lymphocyte and neutrophil infiltration and the excessive keratinization and proliferation of keratinocytes [18,19]. The agents capable of attenuating keratinocyte hyperproliferation and excessive inflammatory responses are considered to be potentially useful for psoriasis treatment [20,21]. IMQ-induced psoriasis is usually accompanied by cellular inflammatory factor disorders in the dorsal skin. As shown in Figure 2A, IMQ induced massive inflammatory cell infiltration in the dorsal skin, which was reduced by CVD and KSCF treatment. As shown in Figure 2B, after 5 days of IMQ treatment, the levels of IL-1β, IL-6, IL-8, IL-17A, IL-22, IL-23, and TNF-α significantly increased in the dorsal skin ($p < 0.05$), whereas IL-10 levels significantly decreased ($p < 0.0001$). After treatment with CVD and KSCF, the levels of IL-1β, IL-6, IL-8, IL-17A, IL-22, IL-23, and TNF-α significantly decreased ($p < 0.05$) and IL-10 levels significantly increased ($p < 0.0001$). These results indicated that KSCF might stimulate the secretion of anti-inflammatory cytokines while inhibiting the release of pro-inflammatory cytokines, thereby alleviating IMQ-induced psoriasis.

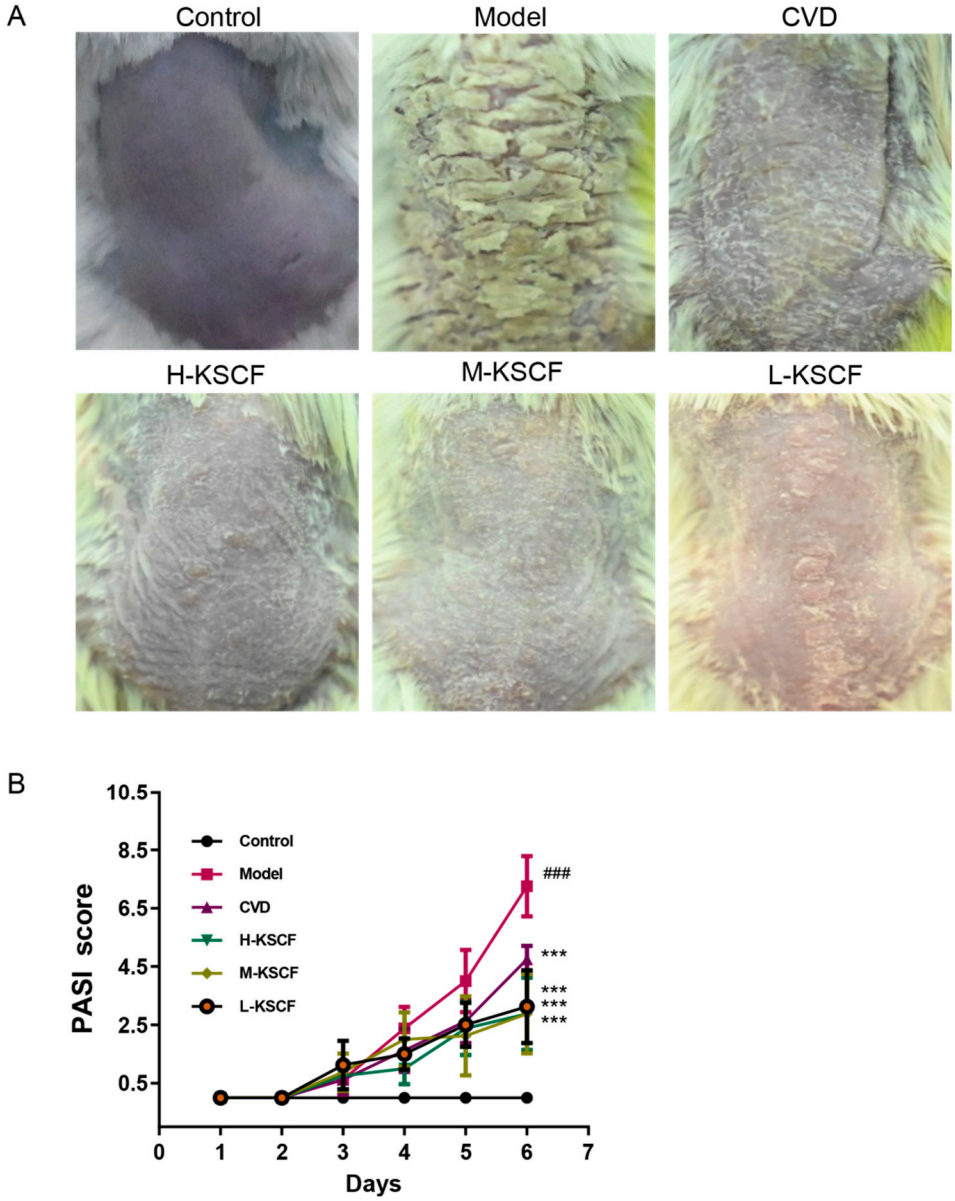


Figure 1. Effect of KSCF on psoriatic dermatitis induced by IMQ. KSCF mitigated skin lesions on the back (**A**) and decreased PASI values (**B**) in IMQ-induced mice. CVD, calcipotriol; H-KSCF, high-dose KSCF group; M-KSCF, medium-dose KSCF group; L-KSCF, low-dose KSCF group. $^{\#}$ vs. control group; * vs. model group; $^{\#\#\#}$ $p < 0.001$; ***$p < 0.001$.

2.3. Effect of KSCF on Metabolites in the Injured Skin of Psoriasis-like Mice

The data of skin samples were collected with ultra-high-performance liquid chromatography/mass spectrometry (UHPLC/MS), and the metabolic profiles of each group were obtained. As depicted in Supplementary Figure S1, the peak number and intensity significantly varied in the total ion current profiles of the control, model, CVD, and KSCF groups, indicating significant differences among the metabolic state of each group and endogenous metabolites. Thus, the endogenous metabolites of skin changed significantly after IMQ induction and administration. In this study, PCA and OPLS-DA were used to analyze metabolome differences in the dorsal skin between the control, model, and KSCF groups using an unsupervised statistical method. The metabolic state of the control and model groups was different (Figures 3 and 4A). The KSCF group was far from the model group. The results demonstrated that KSCF effectively reversed the pathological changes triggered by IMQ treatment in psoriasis-like mice.

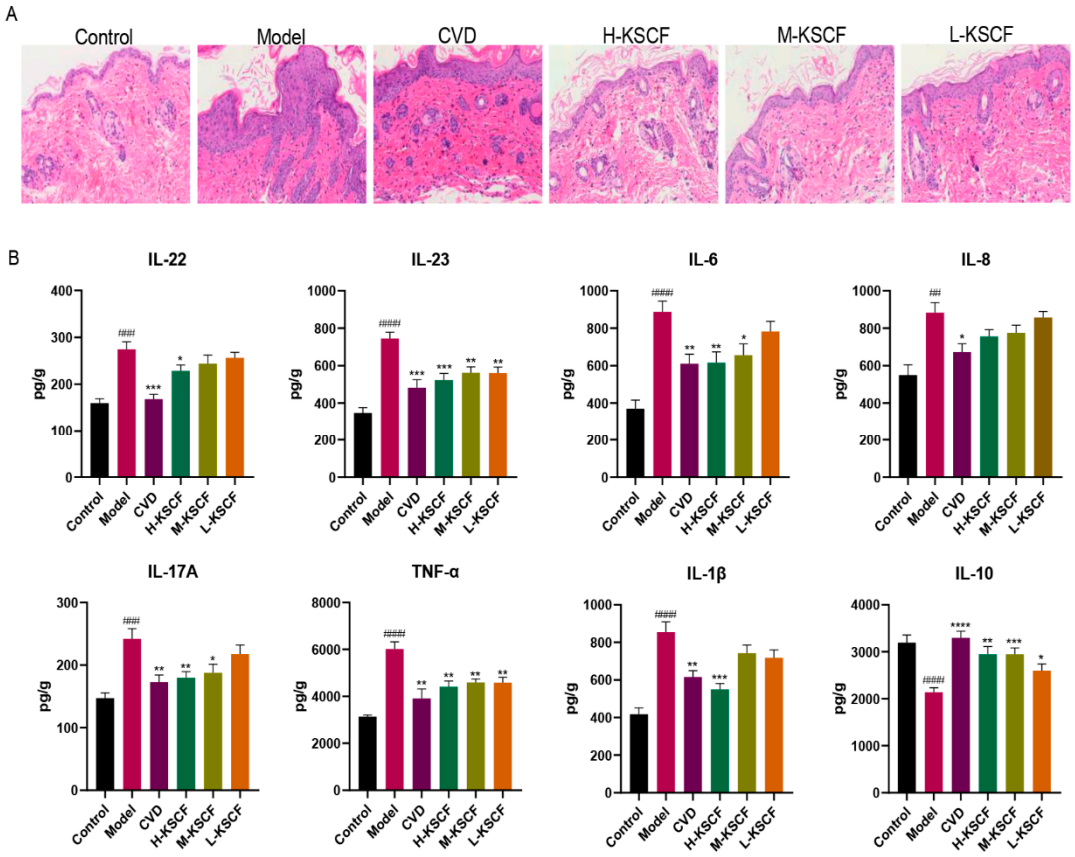


Figure 2. Effect of KSCF on inflammatory reactions in psoriasis−like skin lesions in mice. KSCF reduced inflammatory cell infiltration in the dorsal skin (**A**) and regulated the secretion of inflammatory cytokines (**B**). CVD, calcipotriol group; H-KSCF, high-dose KSCF group; M-KSCF, medium-dose KSCF group; L-KSCF, low-dose KSCF group. # vs. control group; * vs. model group; #### $p < 0.0001$, ### $p < 0.001$, ## $p < 0.01$; **** $p < 0.0001$, *** $p < 0.001$, ** $p < 0.01$, * $p < 0.05$.

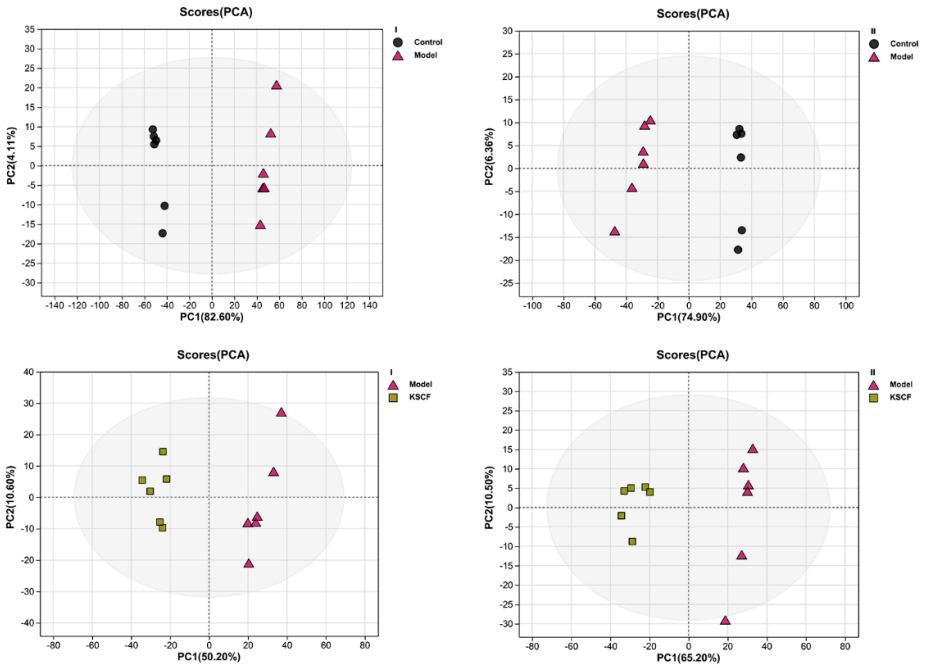


Figure 3. PCA score plots of psoriasis−like skin lesions in mice. I, positive ion mode; II, negative ion mode; KSCF, Kushenol F.

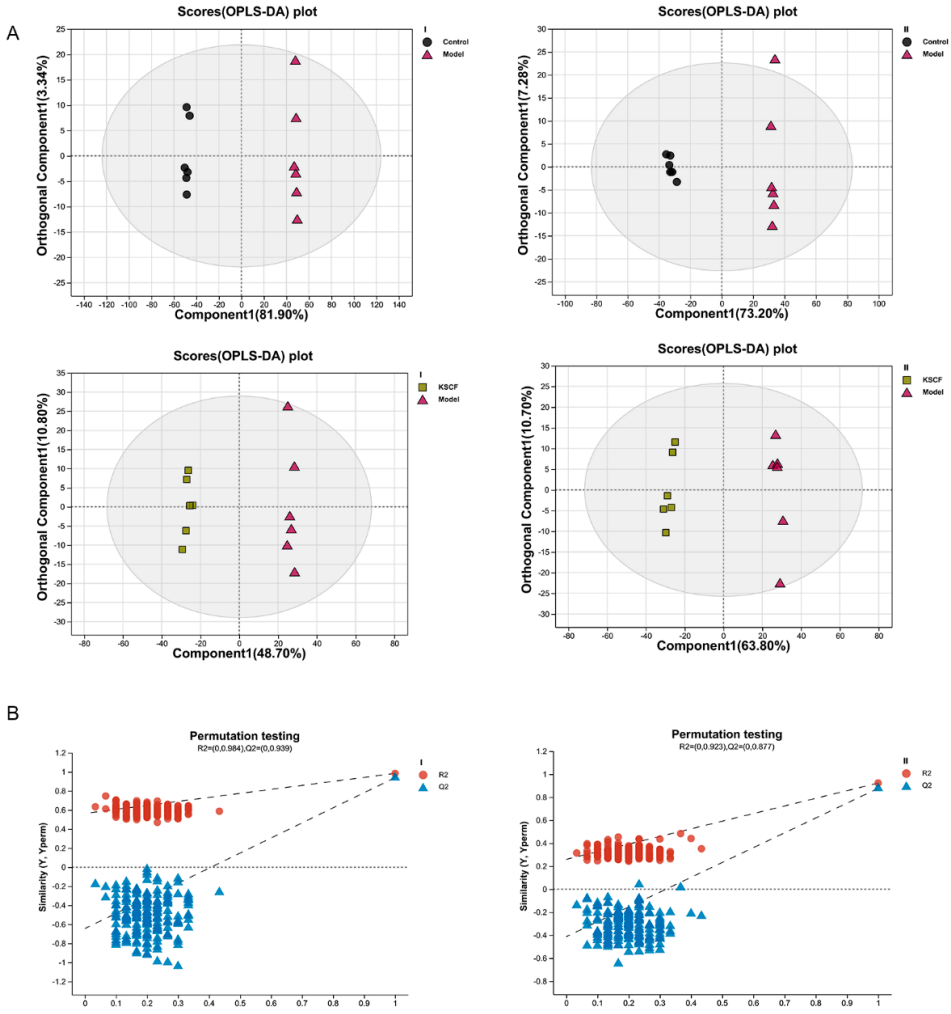


Figure 4. OPLS−DA score plots of psoriasis−like skin lesion samples. (**A**) OPLS−DA score plots. (**B**) Permutation test plot. I, positive ion mode; II, negative ion mode; KSCF, Kushenol F.

Two hundred iteration permutation tests were performed on OPLS-DA in the positive and negative ion modes to further illustrate the reliability of the OPLS-DA model. The Q^2 values were less than 0.05, further confirming the accuracy of the multivariate statistical analysis (Figure 4B).

2.4. Identification of Differential Metabolites

Changes in the metabolites can reflect the physiological and pathological states of the human body and might serve as an objective index to determine the efficacy and mechanism of drugs during disease intervention [22]. The complete metabolic information was collected, and the mechanism of KSCF against IMQ-induced psoriasis, which involved the regulation of endogenous metabolites, was revealed using the UHPLC/MS technique. S-plot diagrams based on OPLS-DA analysis were plotted to obtain information on differential metabolites between the model group and the KSCF group. Substances with a VIP of >1 and *p*-value of <0.05 were selected as biomarkers (Figure 5). A total of 161 potential biomarkers were detected in the dorsal skin, of which 102 metabolites were up-regulated, and 59 metabolites were down-regulated (Table 1; their chemical structures are shown in Supplementary Figure S2). These results suggested that KSCF might regulate these differential metabolites to relieve IMQ-induced psoriasis.

Table 1. Differential metabolites identified from psoriatic skin lesion samples.

Retention Time (min)	Molecular Weight (Da)	VIP	Potential Biomarker	Formula	Change Trend
			ESI−		
4.843	308.124	2.604	Glutaminyltyrosine	$C_{14}H_{19}N_3O_5$	DOWN
6.468	453.202	2.054	2-Hydroxy-imipramine glucuronide	$C_{25}H_{32}N_2O_7$	UP
6.183	581.300	2.676	Serylarginine	$C_9H_{19}N_5O_4$	UP
2.626	263.076	1.478	3,4,5-trihydroxy-6-[(2-methylpropanoyl)oxy]oxane-2-carboxylic acid	$C_{10}H_{16}O_8$	DOWN
2.821	374.095	2.080	7-Hydroxygliclazide	$C_{15}H_{21}N_3O_4S$	DOWN
2.829	299.070	1.075	Methionyl-Glutamate	$C_{10}H_{18}N_2O_5S$	DOWN
4.270	315.163	2.005	3-[8-hydroxy-2-methyl-2-(4-methylpent-3-en-1-yl)-2*H*-chromen-5-yl]propanoic acid	$C_{19}H_{24}O_4$	DOWN
4.791	165.059	1.301	3-Mercapto-2-methyl-1-butanol	$C_5H_{12}OS$	DOWN
6.240	480.249	2.770	Dynorphin A (6–8)	$C_{18}H_{37}N_9O_4$	UP
6.278	457.197	2.666	Deoxypyridinoline	$C18H28N_4O_7$	UP
6.308	469.161	2.372	Melleolide B	$C_{24}H_{32}O_7$	UP
6.308	667.171	1.090	Hydroxychlorpromazine	$C_{17}H_{19}ClN_2OS$	UP
6.347	455.181	2.248	Armillane	$C_{23}H_{32}O_7$	UP
6.378	437.170	2.123	Nevskin	$C_{24}H_{32}O_5$	UP
6.431	177.023	1.656	3,3′-Thiobispropanoic acid	$C_6H_{10}O_4S$	UP
6.442	295.031	2.518	Cis,trans-5′-Hydroxythalidomide	$C_{13}H_{10}N_2O_5$	UP
6.456	421.175	2.033	Euglobal IIb	$C_{23}H_{30}O_5$	UP
6.462	465.202	1.909	Homofukinolide	$C_{25}H_{34}O_6$	UP
6.493	486.187	1.533	4-Hydroxyvalsartan	$C_{24}H_{29}N_5O_4$	UP
5.583	451.185	1.071	7-[(2,6-dihydroxy-2,5,5,8a-tetramethyl-decahydronaphthalen-1-yl)methoxy]-6-hydroxy-2H-chromen-2-one	$C_{24}H_{32}O_6$	UP
6.601	467.217	2.471	Colupdox a	$C_{25}H_{36}O_6$	UP
6.630	553.297	1.078	Phytolaccinic acid	$C_{31}H_{48}O_6$	DOWN
6.969	492.117	2.575	2-amino-4-({1-[(carboxymethyl)-C-hydroxycarbonimidoyl]-2-[(2,3-dihydroxy-1-phenylpropyl)sulfanyl]ethyl}-C-hydroxycarbonimidoyl)butanoic acid	$C_{19}H_{27}N_3O_8S$	UP

Table 1. *Cont.*

Retention Time (min)	Molecular Weight (Da)	VIP	Potential Biomarker	Formula	Change Trend
7.023	609.361	1.208	Lactapiperanol C	$C_{16}H_{26}O_4$	DOWN
7.434	810.583	1.023	PE(18:0/20:0)	$C_{43}H_{86}NO_8P$	DOWN
7.480	606.500	2.048	1,1′-(1,4-Dihydro-4-nonyl-3,5-pyridinediyl)bis[1-dodecanone]	$C_{38}H_{69}NO_2$	DOWN
8.936	453.202	1.579	Colupox a	$C_{25}H_{36}O_5$	UP
8.915	701.421	1.880	PG(a-13:0/a-15:0)	$C_{34}H_{67}O_{10}P$	UP
8.846	465.314	1.130	(2β,3α,9α,24R)-Ergosta-7,22-diene-2,3,9-triol	$C_{28}H_{46}O_3$	DOWN
7.712	865.522	1.182	PG(18:1(11Z)/22:6(4Z,7Z,10Z,13Z,16Z,19Z))	$C_{46}H_{77}O_{10}P$	DOWN
7.365	820.589	1.091	PE(18:1(11Z)/22:1(13Z))	$C_{45}H_{86}NO_8P$	DOWN
7.157	463.293	2.768	Palmitoyl glucuronide	$C_{22}H_{42}O_7$	DOWN
7.057	361.174	0.993	Perindoprilat	$C_{17}H_{28}N_2O_5$	DOWN
6.541	379.218	2.167	3′-Hydroxystanozolol	$C_{21}H_{32}N_2O_2$	DOWN
6.475	439.185	2.144	Lucidone A	$C_{24}H_{34}O_5$	UP
6.456	423.154	2.463	5,7-dihydroxy-4-(1-hydroxypropyl)-6-(3-methylbut-2-en-1-yl)-8-(2-methylbutanoyl)-2H-chromen-2-one	$C_{22}H_{28}O_6$	UP
6.451	455.217	2.656	Cavipetin D	$C_{25}H_{38}O_5$	UP
6.431	475.163	2.153	α-CEHC glucuronide	$C_{22}H_{30}O_{10}$	UP
6.378	500.167	2.330	2-amino-4-({1-[(carboxymethyl)-*C*-hydroxycarbonimidoyl]-2-{[4-(2,6-dihydroxyphenyl)-3-hydroxy-2-methylbutan-2-yl]sulfanyl}ethyl}-*C*-hydroxycarbonimidoyl)butanoic acid	$C_{21}H_{31}N_3O_9S$	UP
6.371	453.165	2.610	Diosbulbin H	$C_{23}H_{30}O_7$	UP
6.354	439.186	1.945	1α-O-Methylquassin	$C_{23}H_{32}O_6$	UP
6.347	507.174	2.465	L-Nicotianine	$C_{10}H_{12}N_2O_4$	UP
6.284	520.193	2.082	Hydroxynefazodone	$C_{25}H_{32}C_1N_5O_3$	UP
6.240	452.218	1.926	Chondroitin sulfate E (GalNAc4,6diS-GlcA), precursor 5a	$C_7H_9N_3O$	UP
6.222	369.211	1.248	3-keto-Digoxigenin	$C_{23}H_{32}O_5$	DOWN
6.218	476.279	1.123	LysoPE(0:0/18:2(9Z,12Z))	$C_{23}H_{44}NO_7P$	DOWN
6.134	457.160	1.105	Valechlorin	$C_{22}H_{31}C_1O_8$	UP
5.718	371.226	2.685	Digoxigenin	$C_{23}H_{34}O_5$	DOWN

Table 1. *Cont.*

Retention Time (min)	Molecular Weight (Da)	VIP	Potential Biomarker	Formula	Change Trend
5.114	348.156	1.934	(+)-O-Methylarmepavine	$C_{20}H_{25}NO_3$	DOWN
5.065	329.179	2.313	12,20-Dioxo-leukotriene B4	$C_{20}H_{28}O_5$	DOWN
4.974	357.211	1.896	17-Hydroxy-E4-neuroprostane	$C_{22}H_{32}O_5$	DOWN
4.589	357.222	1.037	Kinetensin 1-3	$C_{15}H_{30}N_6O_4$	UP
2.829	365.143	1.110	Valproic acid glucuronide	$C_{14}H_{24}O_8$	DOWN
2.814	296.106	1.004	7-Aminonitrazepam	$C_{15}H_{13}N_3O$	DOWN
1.685	295.040	1.398	*N*-Acetyldjenkolic acid	$C_9H_{16}N_2O_5S_2$	UP
1.527	183.044	1.218	Mevalonic acid	$C_6H_{12}O_4$	UP
6.371	383.161	1.501	21-Hydroxy-5b-pregnane-3,11,20-trione	$C_{21}H_{30}O_4$	DOWN
6.278	581.263	1.973	*S*-(3-Methylbutanoyl)-dihydrolipoamide-*E*	$C_{13}H_{25}NO_2S_2$	UP
8.922	689.351	1.131	Zeranol	$C_{18}H_{26}O_5$	UP
			ESI+		
6.444	453.200	3.257	Pro Ser Ser Tyr	$C_{20}H_{28}N_4O_8$	UP
4.727	828.534	0.976	3-*O*-Sulfogalactosylceramide (d18:1/18:1(9Z))	$C_{42}H_{79}NO_{11}S$	DOWN
3.285	404.222	1.210	Ser Ala Ala Arg	$C_{15}H_{29}N_7O_6$	UP
4.253	317.177	1.919	Capillartemisin A	$C_{19}H_{24}O_4$	DOWN
5.069	331.193	2.827	16-Hydroxy-4-oxoretinoic acid	$C_{20}H_{26}O_4$	DOWN
6.224	371.225	1.960	17-phenyl trinor-13,14-dihydro Prostaglandin A2	$C_{23}H_{30}O_4$	DOWN
6.254	395.252	1.328	(3*R*, 6′*Z*)-3,4-Dihydro-8-hydroxy-3-(6-pentadecenyl)-1H-2-benzopyran-1-one	$C_{24}H_{36}O_3$	UP
6.304	565.350	1.002	PG(22:2(13Z,16Z)/0:0)	$C_{28}H_{53}O_9P$	UP
6.324	313.077	2.457	Inosine-5′-carboxylate	$C_{11}H_{12}N_4O_7$	UP
7.031	626.533	1.139	Muricatenol	$C_{37}H_{68}O_6$	UP
6.338	301.077	2.967	Temazepam	$C_{16}H_{13}C_1N_2O_2$	UP
1.543	286.157	2.191	Tryptophyl-Valine	$C_{16}H_{21}N_3O_3$	UP
3.194	298.150	1.266	Histidinyl-Threonine	$C_{10}H_{16}N_4O_4$	DOWN
3.319	281.119	1.191	6-hydroxy-7E,9E-Octadecadiene-11,13,15,17-tetraynoic acid	$C_{18}H_{16}O_3$	UP
4.064	534.323	1.347	Cys Lys Lys Arg	$C_{21}H_{43}N_9O_5S$	DOWN
4.235	255.129	1.186	Isoleucyl-Threonine	$C_{10}H_{20}N_2O_4$	DOWN
4.305	622.377	1.446	Tyr Arg Lys Arg	$C_{27}H_{47}N_{11}O_6$	DOWN
4.474	277.124	1.256	Isobutyrylcarnitine	$C_{11}H_{22}NO_4^+$	UP

Table 1. *Cont.*

Retention Time (min)	Molecular Weight (Da)	VIP	Potential Biomarker	Formula	Change Trend
4.604	386.246	1.473	Pseudoginsenoside RT3	$C_{41}H_{70}O_{13}$	DOWN
4.654	549.172	1.514	Myricatomentoside I	$C_{26}H_{32}O_{10}$	DOWN
4.987	359.225	1.475	7,8-epoxy-17S-HDHA	$C_{22}H_{30}O_4$	DOWN
5.118	696.452	1.502	PA(16:1(9Z)/15:0)	$C_{34}H_{65}O_8P$	DOWN
5.170	828.533	1.338	PE(MonoMe(11,3)/MonoMe(11,3))	$C_{43}H_{74}NO_{10}P$	DOWN
5.994	242.134	0.972	Lysyl-Methionine	$C_{11}H_{23}N_3O_3S$	UP
6.016	548.287	1.511	11-Hydroxyprogesterone 11-glucuronide	$C_{27}H_{38}O_9$	UP
6.082	465.259	1.132	(−)-Jolkinol B	$C_{29}H_{36}O_5$	UP
6.136	502.163	2.001	3-(3-hydroxyphenyl)-2-(4-hydroxyphenyl)-5-[(*E*)-2-(3hydroxyphenyl)ethenyl]-2,3-dihydro-1 benzofuran-6-ol	$C_{28}H_{22}O_5$	UP
6.149	467.275	1.316	1,25-Dihydroxyvitamin D3-26,23-lactone	$C_{27}H_{40}O_5$	UP
6.205	363.225	1.097	5α-Pregnan-20α-ol-3-one	$C_{21}H_{34}O_2$	UP
6.224	453.221	1.813	Australigenin	$C_{27}H_{42}O_4$	UP
6.283	534.221	1.608	Cyclocalopin D	$C_{23}H_{32}O_{13}$	UP
6.297	365.241	1.267	Adipostatin A	$C_{21}H_{36}O_2$	UP
6.324	574.253	1.565	Glaucarubolone 15-*O*-β-D-glucopyranoside	$C_{26}H_{36}O_{13}$	UP
6.360	427.276	1.508	Asymmetric dimethylarginine	$C_8H_{18}N_4O_2$	UP
6.360	455.179	3.227	Gly Glu Ser Tyr	$C_{19}H_{26}N_4O_9$	UP
6.367	441.200	4.192	Gly Thr Tyr Thr	$C_{19}H_{28}N_4O_8$	UP
6.416	435.294	2.760	Alanyl-Lysine	$C_9H_{19}N_3O_3$	UP
6.437	527.345	2.800	Pro Val Arg Arg	$C_{22}H_{42}N_{10}O_5$	UP
6.451	355.125	2.024	Meta-*O*-Dealkylated flecainide	$C_{15}H_{19}F_3N_2O_3$	UP
6.472	463.182	2.851	PA(8:0/8:0)	$C_{19}H_{37}O_8P$	UP
6.479	441.200	3.151	(9*S*,10*S*)-10-hydroxy-9-(phosphonooxy)octadecanoate	$C_{18}H_{37}O_7P$	UP
6.500	714.509	1.058	PA(18:1(9Z)/18:3(9Z,12Z,15Z))	$C_{39}H_{69}O_8P$	UP
6.521	523.411	2.648	Panaxydol linoleate	$C_{35}H_{54}O_3$	DOWN
6.604	411.225	1.903	Pro Pro Thr Pro	$C_{19}H_{30}N_4O_6$	UP
6.646	722.519	1.386	PE(18:4(6Z,9Z,12Z,15Z)/P-18:1(11Z))	$C_{41}H_{72}NO_7P$	UP
6.660	678.492	1.312	PE(18:4(6Z,9Z,12Z,15Z)/P-16:0)	$C_{39}H_{70}NO_7P$	UP
6.674	634.465	1.471	Tsugarioside B	$C_{37}H_{60}O_7$	UP
6.856	670.523	1.605	PE(15:0/18:0)	$C_{38}H_{76}NO_8P$	UP
7.010	904.712	1.184	PC(o-20:0/22:0)	$C_{50}H_{102}NO_7P$	UP
7.066	407.153	1.119	3b,16a-Dihydroxyandrostenone sulfate	$C_{19}H_{28}O_6S$	UP

Table 1. *Cont.*

Retention Time (min)	Molecular Weight (Da)	VIP	Potential Biomarker	Formula	Change Trend
8.944	425.205	4.129	*O*-Desmethylcarvedilol	$C_{23}H_{24}N_2O_4$	UP
9.287	423.189	2.131	Cys Val Thr Thr	$C_{16}H_{30}N_4O_7S$	UP
8.685	895.754	1.939	TG(18:1(11Z)/22:4(7Z,10Z,13Z,16Z)/18:3(9Z,12Z,15Z))	$C_{61}H_{102}O_6$	DOWN
6.940	539.360	1.721	3-methyl-4-(methylamino)-1,2-diphenylbutan-2-ol	$C_{18}H_{23}NO$	UP
6.870	626.496	1.675	PE(15:0/P-16:0)	$C_{36}H_{72}NO_7P$	UP
6.870	614.353	1.399	LysoPC(22:2(13Z,16Z))	$C_{30}H_{58}NO_7P$	UP
6.849	714.550	1.546	PC(14:1(9Z)/18:0)	$C_{40}H_{78}NO_8P$	UP
6.828	802.604	1.578	PC(18:0/22:4(7Z,10Z,13Z,16Z))	$C_{48}H_{88}NO_8P$	UP
6.737	696.496	1.312	CL(i-12:0/18:2(9Z,11Z)/i-18:0/i-19:0)	$C_{76}H_{144}O_{17}P_2$	UP
6.730	740.523	1.185	CL(18:0/18:0/16:1(9Z)/22:6(4Z,7Z,10Z,13Z,16Z,19Z))	$C_{83}H_{148}O_{17}P_2$	UP
6.646	840.578	1.939	PG(18:0/22:4(7Z,10Z,13Z,16Z))	$C_{46}H_{83}O_{10}P$	DOWN
6.604	163.076	1.060	4-Hydroxy-2,6,6-trimethyl-3-oxo-1,4-cyclohexadiene-1-carboxaldehyde	$C_{10}H_{12}O_3$	UP
6.590	295.066	1.816	2-hydroxy-3-[3-(3-methylbut-2-en-1-yl)-4-(sulfooxy)phenyl]propanoic acid	$C_{14}H_{18}O_7S$	UP
6.583	459.187	2.136	Ser Glu Ser His	$C_{17}H_{26}N_6O_9$	UP
6.542	355.194	1.101	Nigakihemiacetal B	$C_{22}H_{30}O_6$	DOWN
6.493	764.516	1.715	CL(16:0/18:0/18:0/22:5(7Z,10Z,13Z,16Z,19Z))	$C_{83}H_{152}O_{17}P_2$	DOWN
6.472	700.493	1.413	PA(15:0/18:2(9Z,12Z))	$C_{36}H_{67}O_8P$	UP
6.472	385.136	3.206	2′,7-Dihydroxy-4′-methoxy-8-prenylflavan	$C_{21}H_{24}O_4$	UP
6.465	351.130	1.754	N-Ribosylhistidine	$C_{11}H_{17}N_3O_6$	UP
6.451	521.396	1.727	Ginsenoyne A linoleate	$C_{35}H_{52}O_3$	DOWN
6.388	285.081	1.654	(2*S*)-2-hydrazinyl-3-(4-hydroxy-3-methoxyphenyl)-2-methylpropanoic acid	$C_{11}H_{16}N_2O_4$	DOWN
6.381	439.184	3.069	Gln Glu Tyr	$C_{19}H_{26}N_4O_8$	UP
6.345	375.115	1.271	Cyclic *N*-Acetylserotonin glucuronide	$C_{18}H_{20}N_2O_8$	DOWN
6.338	361.135	2.023	7-Hydroxy-6-methyl-8-ribityl lumazine	$C_{12}H_{16}N_4O_7$	UP
6.324	538.255	1.523	Rubraflavone B	$C_{30}H_{34}O_5$	UP
6.311	618.283	2.136	3′-Deaminofusarochromanone	$C_{15}H_{19}NO_4$	UP
6.297	424.221	2.812	Sphingosine 1-phosphate	$C_{18}H_{38}NO_5P$	UP
6.290	508.280	2.746	LysoPE(0:0/22:6(4Z,7Z,10Z,13Z,16Z,19Z))	$C_{27}H_{44}NO_7P$	UP
6.283	510.296	4.312	LysoPE(0:0/22:5(7Z,10Z,13Z,16Z,19Z))	$C_{27}H_{46}NO_7P$	UP
6.276	583.277	3.375	(4*E*)-6-hydroxy-1,7-diphenylhept-4-en-3-one	$C_{19}H_{20}O_2$	UP

Table 1. *Cont.*

Retention Time (min)	Molecular Weight (Da)	VIP	Potential Biomarker	Formula	Change Trend
6.241	451.279	0.944	PA(19:1(9Z)/0:0)	$C_{22}H_{43}O_7P$	UP
6.231	498.259	3.159	PE(18:3/0:0)	$C_{23}H_{42}NO_7P$	UP
6.199	437.264	1.065	1-Oleoyl Lysophosphatidic Acid (sodium salt)	$C_{21}H_{41}O_7P$	UP
6.186	175.123	2.811	α-Methyltryptamine (AMT)	$C_{11}H_{14}N_2$	UP
6.174	569.298	3.370	11-α-*O*-β-D-Glucopyranosyl-16α-*O*-methylneoquassin	$C_{29}H_{44}O_{11}$	UP
6.075	487.359	1.085	Lys Ile Val Lys	$C_{23}H_{46}N_6O_5$	UP
6.005	618.340	1.903	Pentasine	$C_{30}H_{49}N_6O_{10}^+$	UP
6.000	349.209	1.127	Oryzalexin E	$C_{20}H_{32}O_2$	UP
5.554	183.082	1.526	2-Methyl-4-propyl-1,3-oxathiane	$C_8H_{16}OS$	UP
5.112	740.479	1.500	PS(14:0/20:3(8Z,11Z,14Z))	$C_{40}H_{72}NO_{10}P$	DOWN
5.006	240.142	0.993	Isopropyl β-D-glucoside	$C_9H_{18}O_6$	UP
4.945	336.130	0.976	Gynocardin	$C_{12}H_{17}NO_8$	DOWN
4.897	352.161	1.890	(+/−)-Rollipyrrole	$C_{16}H_{20}N_2O_3$	DOWN
4.615	338.145	1.145	*N*-Acetyl-3-hydroxyprocainamide	$C_{15}H_{23}N_3O_3$	DOWN
4.391	233.097	1.094	L-Targinine	$C_7H_{16}N_4O_2$	UP
3.611	402.242	1.022	*N*-Didesmethylmifepristone (RU 42848)	$C_{27}H_{31}NO_2$	DOWN
3.396	261.150	1.327	Methyl dihydrophaseate	$C_{16}H_{24}O_5$	UP
3.222	229.123	1.660	Blennin B	$C_{15}H_{20}O_4$	UP
2.566	267.140	1.527	(*S*)-17-Hydroxy-9,11,13,15-octadecatetraynoic acid	$C_{18}H_{20}O_3$	UP
1.360	217.134	1.518	Girgensonine	$C_{13}H_{16}N_2O$	DOWN
0.013	300.208	1.040	2-hydroxydesipramine	$C_{18}H_{22}N_2O$	UP
6.800	524.283	1.270	11-β-Hydroxyandrosterone-3-glucuronide	$C_{25}H_{38}O_9$	UP

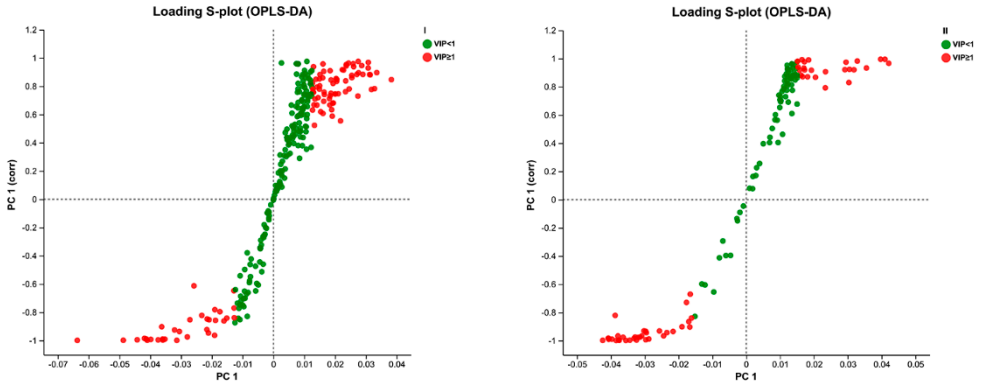


Figure 5. S−Plot of the model and KSCF administration group. I, positive ion mode; II: negative ion mode; red, VIP $\geq$ 1; green, VIP < 1.

2.5. Metabolic Pathway Analysis

The differential metabolites were subjected to a pathway enrichment analysis to explore the potential metabolic pathways of KSCF exerting medicinal effects. Figure 6 shows the path influence diagrams of the metabolic pathway analysis. Pathways with a *p*-value of <0.05 were considered KSCF-involved pathways. The difference between the model and KSCF groups was clearly reflected in three pathways (Table 2), which are mainly related to lipid metabolism and steroidogenic activity.

Sphingolipids have structural and biological functions in the human epidermis, are importantly involved in the maintenance of the skin barrier, and regulate cellular processes, such as the proliferation, differentiation, and apoptosis of keratinocytes [23,24]. In this study, 3-O-sulfogalactosylceramide (d18:1/18:1(9Z)) and sphingosine 1-phosphate were identified as metabolites with significant differences after modeling and drug administration, suggesting that these key metabolites could be targets for KSCF against IMQ-induced psoriasis. Therefore, it was inferred that KSCF improved IMQ-induced psoriasis by regulating sphingolipid metabolism pathways.

Abnormal linoleic acid metabolism has been shown to be a key pathway in psoriasis. The combination of a moisturizer containing a linoleic acid–ceramide complex and glucocorticoids was shown to significantly improve the therapeutic efficacy of psoriasis and delay recurrence [25]. Our results confirmed that the levels of PC (14:1(9Z)/18:0) and PC (18:0/22:4(7Z,10Z,13Z,16Z)) were close to the normal group after KSCF administration. These results suggested that KSCF improved IMQ-induced psoriasis by regulating the linoleic acid metabolism pathways.

The skin has an endogenous steroidogenic capacity, and modulating local steroidogenic activity may be a new approach to treating inflammatory skin diseases [26,27]. In this study, 5α-Pregnan-20α-ol-3-one and 21-Hydroxy-5b-pregnane-3,11,20-trione were identified as metabolites with significant differences after modeling and drug administration. After KSCF administration, steroid hormone biosynthesis was similar to the normal group, suggesting that KSCF treatment affected steroid hormone biosynthesis to relieve IMQ-induced psoriasis.

Our results indicated that KSCF inhibited the inflammatory response to prevent IMQ-induced psoriasis-like skin lesions in mice by call-backing the levels of endogenous metabolites and affecting their related metabolic pathways (Figure 7). It is very likely that the flavonoid extract from *S. flavescens* also shows the therapeutic effects on psoriasis because it contains many active compounds, such as KSCF, which is worthy of further study. The deep molecular mechanism of KSCF regulating endogenous metabolites in three key pathways is also worthy to be further explored by detecting the key proteins in the pathways. It is reported that another flavonoid (kurarinone) and alkaloids (matrine and oxymarine) isolated from *S. flavescens* regulated the inflammatory response to intervene in psoriasis [7,28,29]. However, the differences in the efficacy and mechanism of these

compounds in the psoriasis treatment and the relationship between the chemical structures of them and their anti-psoriasis activity are still unclear, which is worthy of further study.

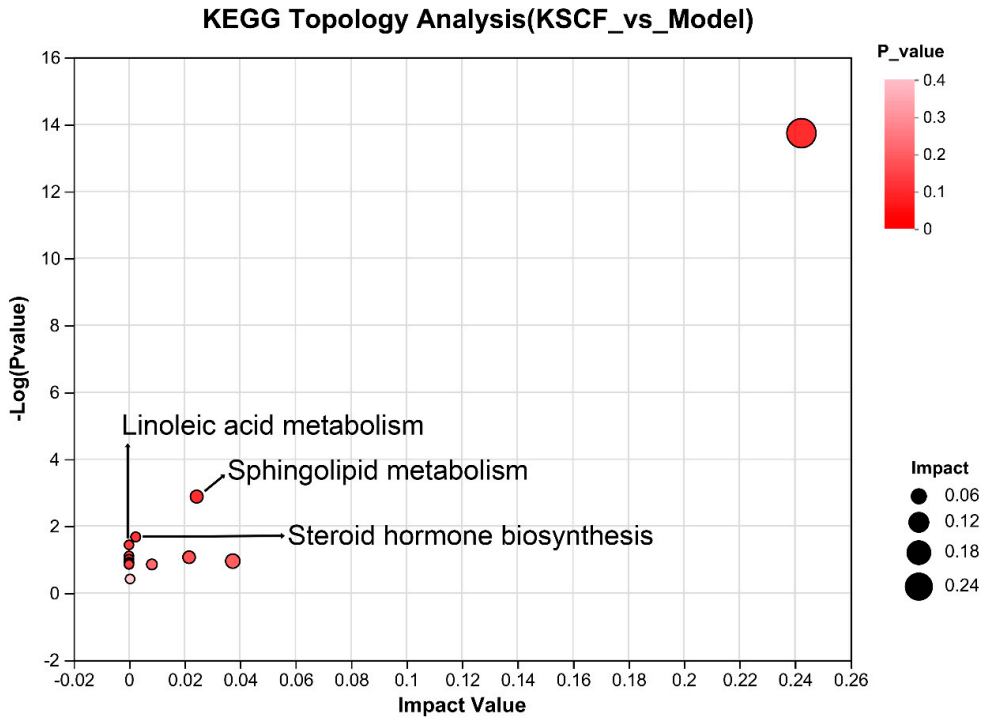


Figure 6. Pathway analysis of KSCF treatment.

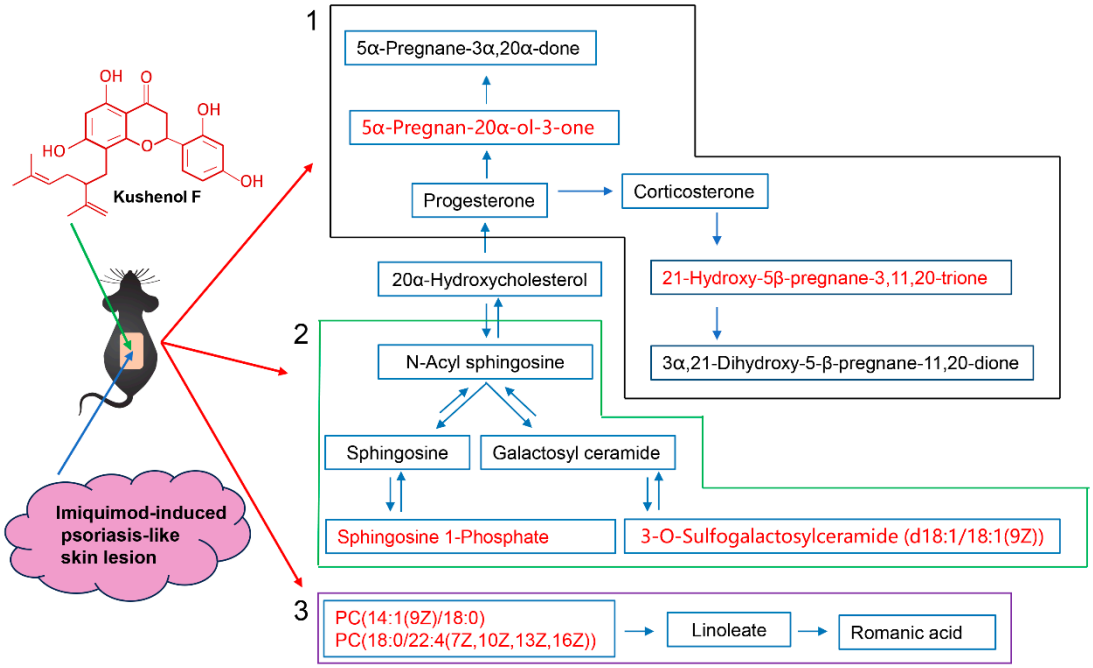


Figure 7. KSCF regulated endogenous metabolites in three key pathways against IMQ-induced psoriasis. 1, steroid hormone biosynthesis; 2, sphingolipid metabolism; 3, linoleic acid metabolism. Red, up.

Table 2. Metabolic pathway of psoriatic skin lesion samples.

No.	Pathway	*p*-Value	Details
1	Sphingolipid metabolism	0.001	KEGG
2	Linoleic acid metabolism	0.036	KEGG
3	Steroid hormone biosynthesis	0.021	KEGG

3. Materials and Methods

3.1. Chemicals, Reagents, and Materials

KSCF was provided from Chengdu Pufei De Biotech Co., Ltd. (Chengdu, China). CVD was purchased from A&M Pharmaceuticals (Hong Kong, China). Hematoxylin stain was obtained from Wuhan Google Biotechnology Co., Ltd. (Wuhan, China). Vaseline for medical use was purchased from Shandong Lircon Medical Technology Co., Ltd. (Dezhou, China). IMQ was acquired from Sichuan MED-SHINE Pharmaceutical Co., Ltd. (Chengdu, China). Four percent paraformaldehyde solution was provided from Beijing lanjieke Technology Co., Ltd. (Beijing, China). IL-6, IL-8, IL-1β, IL-10, IL-22, IL-23, IL-17A, and TNF-α ELISA Kits were purchased from Jiangsu Meimian Industrial Co., Ltd. (Yancheng, China). The reference substance of KSCF (purity > 98%) was purchased from Chengdu Pufei De Biotech Co., Ltd. (Chengdu, China). High purity deionized water was purified using a Milli-Q system (Millipore, Bedford, MA, USA). HPLC-grade formic acid, methyl alcohol, and acetonitrile were acquired from Fischer Control Equipment International Co., Ltd. (Hong Kong, China). H&E Staining kits were purchased from Beijing Solarbio Science&Technology Co., Ltd. (Beijing, China). Seventy-five percent ethanol was purchased from Sinopharm Chemical Reagent Co., Ltd. (Shanghai, China). All other reagents used were of analytical reagent grade or higher.

3.2. Animals and Experimental Protocol

All experimental procedures in this study complied with the National Guidelines for the Care and Use of Laboratory Animals and were approved by the Animal Ethics Committee of Yunnan University of Chinese Medicine, with ethics number R062021158.

Healthy male BALB/c mice (20 ± 2 g), aged 6–8 weeks, were obtained from Sipeifu Biotechnology Co., Ltd. (Beijing, China). The mice were kept in the Laboratory of Yunnan University of Traditional Chinese Medicine (Kunming, China), following standard housing conditions. All mice were adaptively fed for one week. The mice were randomized into six groups (n = 6 mice per group), including control group (75% ethanol), model group (75% ethanol), positive group (CVD, 62.5 mg/kg), low-dose KSCF group (L-KSCF, 200 mg/kg), medium-dose KSCF group (M-KSCF, 400 mg/kg), and high-dose KSCF group (H-KSCF, 600 mg/kg). Except for the control group, mice were topically treated with 5% IMQ cream at a daily dose of 62.5 mg for a duration of 5 days on their dorsal region. KSCF and CVD were dissolved in 75% ethanol. Starting from the day of modeling, the corresponding drugs were sprayed continuously for 5 days (0.3 mL/day/mouse) in the administration group. Seventy-five percent ethanol (0.3 mL/day/mouse) was sprayed for the control group and the model group.

3.3. Psoriasis Area and Severity Index (PASI) Assessment

According to clinical PASI score standard, the severity of the skin inflammation was evaluated once daily, including the measurements for skin erythema, scaling, and thickening. Erythema, scaling, and thickening were scored independently on a scale from 0 to 4: 0, none; 1, slight; 2, moderate; 3, marked; 4, very marked. The cumulative score (erythema plus scaling plus thickening) served as a measure of the severity of inflammation (scale 0–12) [30].

3.4. Image Acquisition and Skin Sample Collection

After euthanizing the mice through carbon dioxide asphyxiation, images were captured on the dorsal side of each mouse group. Then, the dorsal skin of the mice was carefully excised using surgical scissors and divided into two sections. One section was immediately immersed in liquid nitrogen for cryopreservation, while the other section was fixed in 4% paraformaldehyde universal tissue fixative.

3.5. Histopathology Analyses

The dorsal skin of mice was fixed in 4% paraformaldehyde universal tissue fixative for 24 h, washed with PBS, dehydrated with gradient ethanol and transparentized with xylene, and embedded in paraffin. After hematoxylin and eosin staining, histological parameters were observed under a light microscope, and images were taken at 200× magnification.

3.6. Measurement of Skin Inflammatory Factors

Approximately 50 mg of injured skin from the dorsal region of each mouse were weighed and placed on ice. The surface blood stains on the skin samples were rinsed with pre-cooled normal saline solution. After air-drying the filter paper, the skin samples were promptly sectioned into pieces and transferred into a covered 2 mL centrifuge tube. The tube was then subjected to centrifugation (Centrifuge 5430R, Eppendorf, Germany) at 1500× *g* for 15 min, and subsequently, the supernatant of the homogenized tissue was collected for further utilization. The levels of cytokines IL-1β, IL-6, IL-8, IL-10, IL-17A, IL-22, IL-23, and TNF-α in the dorsal skin lesions of all groups of mice were detected according to the kit manufacturer's instructions. The values were determined by measuring the absorbance value (OD) at 450 nm using a microplate reader (Rayto Life and Analytical Sciences Co., Ltd., Shenzhen, China).

3.7. Metabolomic Analysis

3.7.1. Sample Pre-Treatment

Skin samples: 50 mg skin sample and a 6 mm diameter grinding bead was added to a 2 mL centrifuge tube. An amount of 400 µL of extraction solution (methanol: water = 4:1 (*v*:*v*)) was used for metabolite extraction. Samples were ground with Wonbio-96c frozen tissue grinder (Shanghai Wanbo Biotechnology Co., Ltd., Shanghai, China) for 6 min (−10 °C, 50 Hz) followed by low-temperature ultrasonic extraction for 30 min (5 °C, 40 kHz). Then, the sample was allowed to stand for 30 min at −20 °C and centrifuged for 15 min (4 °C, 3500× *g*). The supernatant was transferred to a clean tube and dried gently with nitrogen. The residues were redissolved in 200 µL of methanol for UHPLC/MS analysis.

Quality control sample: A random injection sequence was employed to detect signal fluctuation. An amount of 2 µL of skin samples were taken and thoroughly mixed. Then, the mixture was centrifuged at 3500× *g* for 15 min at 4 °C. The supernatant was collected to perform UHPLC/MS analysis.

3.7.2. UHPLC/MS Analysis

UHPLC analyses were performed using Ultimate 3000 Ultra High Performance Liquid Chromatography (Thermo Fisher Scientific, San Jose, CA, USA) equipped with a Thermo Scientific Hypersil GOLD column (50 mm × 2.1 mm, 1.9 µm). The column temperature was maintained at 40 °C to obtain better sample separation. The mobile phases consisted of water containing 0.1% formic acid (A) and acetonitrile (B) at a 0.4 mL/min of flow rate. The gradient program was set as follows: 0–3.5 min, 0% B → 24.5% B; 3.5–5 min, 24.5% B → 65% B; 5–7.4 min, 65% B → 100% B; 7.4–7.6 min, 100% B → 51.5% B; 7.6–10 min, 51.5% B → 0% B.

The MS data were collected using a Thermo Scientific Q-Exactive TM hybrid quadrupole-orbitrap mass spectrometer with a heated electrospray ionization probe (Thermo Fisher Scientific, San Jose, CA, USA). MS conditions were as follows: CUR, 15 psi; Gas1 and Gas2, 50 psi; IS, 5500 V; gas temperature, 500 °C.

3.8. Statistical Analysis

All UHPLC/MS raw files were exported in comma-separated value (CSV) format using the Progenesis QI (Waters Corporation, Milford, CT, USA) software. All data were uploaded to XCMS online for peak alignment, normalization, and retrieval. The data were analyzed with principal component analysis (PCA) and orthogonal partial least squares discriminant analysis (OPLS-DA) using the SIMCA-P 14.1 software (Sweden, Umeå, Umetrics). The potential biomarkers were selected according to the parameters of variable importance in the projection (VIP > 1 and $p < 0.05$) from OPLS-DA. The structural information of the metabolites was identified using the HMDB databases. Finally, the metabolic pathways were searched using Kyoto Encyclopedia of Genes and Genomes (KEGG) through MetaboAnalyst 5.0 online, and the pathways with an impact value greater than 0.1 were considered KSCF-involved pathways.

All experimental data were presented as means ± S.D. Each experiment was performed in triplicate. The overall significance of the results was examined with one-way ANOVA using GraphPad Prism 5.0 (GraphPad Software, La Jolla, CA, USA). Kolmogorov–Smirnov test was used for the pre-test of the analysis of ANOVA to ensure the rationality of the statistical analysis. Student's *t*-test delivered the *p*-values shown. The differences between the compared groups were considered statistically significant at $p < 0.05$, $p < 0.01$, $p < 0.001$, $p < 0.0001$.

4. Conclusions

KSCF inhibited the inflammatory response to prevent IMQ-induced psoriasis-like skin lesions in mice by call-backing the levels of 161 endogenous metabolites and affecting the three related metabolic pathways, including sphingolipid and linoleic acid metabolism and steroid hormone biosynthesis. Thus, KSCF has the potential to be developed as a topical drug for treating psoriasis.

Supplementary Materials: The following supporting information can be downloaded at: https://www.mdpi.com/article/10.3390/molecules29112410/s1, Figure S1: Representative total ion current profiles of the skin samples in the negative and positive ion mode; Figure S2: The chemical structures of 161 potential biomarkers.

Author Contributions: Z.C. and J.C. wrote the manuscript. J.C., X.Y. (Xunqing Yin) and T.A. performed the experiments. Z.C., Y.Y. and X.H. provided technical support and helpful discussions. Y.Y. and X.Y. (Xingxin Yang) wrote and modified the manuscript. X.Y. (Xingxin Yang) and Y.L. designed the study. All authors have read and agreed to the published version of the manuscript.

Funding: This study was supported by grants from the National Natural Science Foundation of China (Grant numbers 82174037, 82060707, 82104381, and 81960710) and the Application and Basis Research Project of Yunnan China (Grant numbers 202001AV070007, 202001AZ070001-006, 202201AW070016, 2019IB009 and 202101AY070001-077).

Institutional Review Board Statement: All experimental procedures in this study complied with the National Guidelines for the Care and Use of Laboratory Animals and were approved by the Animal Ethics Committee of Yunnan University of Chinese Medicine, with ethics number R062021158.

Informed Consent Statement: Not applicable.

Data Availability Statement: Data are available upon request.

Conflicts of Interest: The authors declare that they have no competing interests.

References

1. Wu, J.J.; Kavanaugh, A.; Lebwohl, M.G.; Gniadecki, R.; Merola, J.F. Psoriasis and metabolic syndrome: Implications for the management and treatment of psoriasis. *J. Eur. Acad. Dermatol. Venereol.* **2022**, *36*, 797–806. [CrossRef] [PubMed]
2. Armstrong, A.W.; Read, C. Pathophysiology, Clinical Presentation, and Treatment of Psoriasis: A Review. *JAMA* **2020**, *19*, 1945–1960. [CrossRef] [PubMed]
3. Lee, H.J.; Kim, M. Challenges and future trends in the treatment of psoriasis. *Int. J. Mol. Sci.* **2023**, *24*, 13313. [CrossRef] [PubMed]

4. Tokuyama, M.; Mabuchi, T. New treatment addressing the pathogenesis of psoriasis. *Int. J. Mol. Sci.* **2020**, *21*, 7488. [CrossRef] [PubMed]
5. Liu, L.; Jin, R.; Hao, J.; Zeng, J.; Yin, D.; Yi, Y.; Zhu, M.; Mandal, A.; Hua, Y.; Ng, C.K.; et al. Consumption of the fish oil high-fat diet uncouples obesity and mammary tumor growth through induction of reactive oxygen species in protumor macrophages. *Cancer Res.* **2020**, *80*, 2564–2574. [CrossRef] [PubMed]
6. Hao, J.; Jin, R.; Zeng, J.; Hua, Y.; Yorek, M.S.; Liu, L.; Mandal, A.; Li, J.; Zheng, H.; Sun, Y.; et al. Consumption of fish oil high-fat diet induces murine hair loss via epidermal fatty acid binding protein in skin macrophages. *Cell Rep.* **2022**, *41*, 111804. [CrossRef] [PubMed]
7. Kim, B.H.; Na, K.M.; Oh, I.; Song, I.H.; Lee, Y.S.; Shin, J.; Kim, T.Y. Kurarinone regulates immune responses through regulation of the JAK/STAT and TCR-mediated signaling pathways. *Biochem. Pharmacol.* **2013**, *85*, 1134–1144. [CrossRef]
8. Griffiths, C.E.M.; Armstrong, A.W.; Gudjonsson, J.E.; Barker, J.N.W.N. Psoriasis. *Lancet* **2021**, *397*, 1301–1315. [CrossRef] [PubMed]
9. Kamata, M.; Tada, Y. Crosstalk: Keratinocytes and immune cells in psoriasis. *Front. Immunol.* **2023**, *14*, 1286344. [CrossRef]
10. Sun, P.; Zhao, W.; Wang, Q.; Chen, L.; Sun, K.; Zhan, Z.; Wang, J. Chemical diversity, biological activities and traditional uses of and important Chinese herb Sophora. *Phytomedicine* **2022**, *100*, 154054. [CrossRef]
11. Zhang, Z.; Pan, J.; Zhu, T.; Malewicz, N.; Ye, K.; Rong, J.; Luo, Y.; Situ, Y.; Verkhratsky, A.; Wang, Y.; et al. Oxymatrine screened from *Sophora flavescens* by cell membrane immobilized chromatography relieves histamine-independent itch. *J. Pharm. Pharmacol.* **2021**, *73*, 1617–1629. [CrossRef] [PubMed]
12. Sun, P.; Zhao, X.; Zhao, W.; Chen, L.; Liu, X.; Zhan, Z.; Wang, J. *Sophora flavescens-Angelica sinensis* in the treatment of eczema by inhibiting TLR4/MyD88/NF-κB pathway. *J. Ethnopharmacol.* **2024**, *322*, 117626. [CrossRef] [PubMed]
13. Cha, J.D.; Moon, S.E.; Kim, J.Y.; Jung, E.K.; Lee, Y.S. Antibacterial activity of sophoraflavanone G isolated from the roots of *Sophora flavescens* against methicillin-resistant staphylococcus aureus. *Phytother. Res.* **2009**, *23*, 1326–1331. [CrossRef]
14. Li, Z.Y.; Huang, W.C.; Tu, R.S.; Gu, P.Y.; Lin, C.F.; Liou, C.J. Sophoraflavanone G induces apoptosis in human leukemia cells and blocks MAPK activation. *Am. J. Chin. Med.* **2016**, *44*, 165–176. [CrossRef] [PubMed]
15. Li, J.; Wei, S.; Marabada, D.; Wang, Z.; Huang, Q. Research progress of natural matrine compounds and synthetic matrine derivatives. *Molecules* **2023**, *31*, 5780. [CrossRef] [PubMed]
16. Tashiro, T.; Sawada, Y. Psoriasis and systemic inflammatory disorders. *Int. J. Mol. Sci.* **2022**, *23*, 4457. [CrossRef]
17. Guo, L.; Jin, H. Research progress of metabolomics in psoriasis. *Chin. Med. J.* **2023**, *136*, 1805–1816. [CrossRef] [PubMed]
18. Kanda, N. Psoriasis: Pathogenesis, comorbidities, and therapy updated. *Int. J. Mol. Sci.* **2021**, *22*, 2979. [CrossRef]
19. Gao, J.; Chen, F.; Fang, H.; Mi, J.; Qi, Q.; Yang, M. Daphnetin inhibits proliferation and inflammatory response in human HaCaT keratinocytes and ameliorates imiquimod-induced psoriasis-like skin lesion in mice. *Biol. Res.* **2020**, *53*, 48. [CrossRef]
20. Fletcher, J.M.; Moran, B.; Petrasca, A.; Smith, C.M. IL-17 in inflammatory skin diseases psoriasis and hidradenitis suppurativa. *Clin. Exp. Immunol.* **2020**, *201*, 121–134. [CrossRef]
21. Elpa, D.P.; Chiu, H.Y.; Wu, S.P.; Urban, P.L. Skin metabolomics. *Trends Endocrinol. Metab.* **2021**, *32*, 66–75. [CrossRef] [PubMed]
22. Hu, X.; Qi, C.; Feng, F.; Wang, Y.; Di, T.; Meng, Y.; Wang, Y.; Zhao, N.; Zhang, X.; Li, P.; et al. Combining network pharmacology, RNA-seq, and metabolomics strategies to reveal the mechanism of cimicifugae rhizome—Smilax glabra roxb herb pair for the treatment of psoriasis. *Phytomedicine* **2022**, *105*, 154384. [CrossRef]
23. Bocheńska, K.; Gabig-Cimińska, M. Unbalanced sphingolipid metabolism and its implications for the pathogenesis of psoriasis. *Molecules* **2020**, *25*, 1130. [CrossRef] [PubMed]
24. Matwiejuk, M.; Mysliwiec, H.; Chabowski, A.; Flisiak, I. The role of sphingolipids in the pathogenesis of psoriasis. *Metabolites* **2022**, *12*, 1171. [CrossRef] [PubMed]
25. Li, X.; Yang, Q.; Zheng, J.; Gu, H.; Chen, K.; Jin, H.; He, C.; Xu, A.E.; Xu, J.; Zhang, J.L.; et al. Efficacy and safety of a topical moisturizer containing linoleic acid and ceramide for mild-to-moderate psoriasis vulgaris: A multicenter randomized controlled trial. *Dermatol. Ther.* **2023**, *33*, e14263. [CrossRef]
26. Slominski, A.; Zbytek, B.; Nikolakis, G.; Manna, P.R.; Skobowiat, C.; Zmijewski, M.; Li, W.; Janjetovic, Z.; Postlethwaite, A.; Zouboulis, C.C.; et al. Steroidogenesis in the skin: Implications for local immune functions. *J. Steroid Biochem. Mol. Biol.* **2013**, *137*, 107–123. [CrossRef] [PubMed]
27. Jin, R.; Luo, L.; Zheng, J. The trinity of skin: Skin homeostasis as a neuro-endocrine-immune organ. *Life* **2022**, *12*, 725. [CrossRef]
28. Li, N.; Zhao, J.; Di, T.; Meng, Y.; Wang, M.; Li, X.; Liu, Z.; Zhai, C.; Zhang, L.; Ma, C.; et al. Matrine alleviates imiquimod-induced psoriasiform dermatitis in BALB/c mice via dendritic cell regulation. *Int. J. Clin. Exp. Pathol.* **2018**, *11*, 5232–5240.
29. Xiang, X.; Tu, C.; Li, Q.; Wang, W.; Huang, X.; Zhao, Z.; Xiong, H.; Mei, Z. Oxymatrine ameliorates imiquimod-induced psoriasis pruritus and inflammation through inhibiting heat shock protein 90 and heat shock protein 60 expression in keratinocytes. *Toxicol. Appl. Pharmacol.* **2020**, *405*, 115209. [CrossRef]
30. Jiang, W.W.; Wang, Y.M.; Wang, X.Y.; Zhang, Q.; Zhu, S.M.; Zhang, C.L. Role and mechanism of matrine alone and combined with acitretin for HaCaT cells and psoriasis-like murine models. *Chin. Med. J.* **2019**, *132*, 2079–2088. [CrossRef]

Disclaimer/Publisher's Note: The statements, opinions and data contained in all publications are solely those of the individual author(s) and contributor(s) and not of MDPI and/or the editor(s). MDPI and/or the editor(s) disclaim responsibility for any injury to people or property resulting from any ideas, methods, instructions or products referred to in the content.